NJC

Accepted Manuscript

This is an *Accepted Manuscript*, which has been through the Royal Society of Chemistry peer review process and has been accepted for publication.

Accepted Manuscripts are published online shortly after acceptance, before technical editing, formatting and proof reading. Using this free service, authors can make their results available to the community, in citable form, before we publish the edited article. We will replace this *Accepted Manuscript* with the edited and formatted *Advance Article* as soon as it is available.

You can find more information about *Accepted Manuscripts* in the **Information for Authors**.

Please note that technical editing may introduce minor changes to the text and/or graphics, which may alter content. The journal's standard **Terms & Conditions** and the **Ethical guidelines** still apply. In no event shall the Royal Society of Chemistry be held responsible for any errors or omissions in this *Accepted Manuscript* or any consequences arising from the use of any information it contains.

Self- assembly, photophysical, electrochemical properties and activation of TiO₂ photocatalyst by perylene bisimide

Adhimoolam Senthilraja[a], BaluKrishnakumar[a], Meenankshisundaram Swaminathan[a] and Samuthira Nagarajan[b]*

[a]Department of Chemistry, Annamalai University, Annamalainagar 608 002, Tamil Nadu, India.
[b]Department of Chemistry, Central University of Tamil Nadu, Thiruvarur 601101, Tamil Nadu, India.

*Corresponding author:
S. Nagarajan
Associate Professor
Department of Chemistry
Central University of Tamil Nadu
Thiruvarur 610 101
India.
E -mail:snagarajan@cutn.ac.in
Tel: +91 94430 46272

Self- assembly, photophysical, electrochemical properties and activation of TiO$_2$ photocatalyst by perylene bisimide

Adhimoolam Senthilraja[a], Balu Krishnakumar[a], Meenankshisundaram Swaminathan[a] and Samuthira Nagarajan[b]*

[a]Department of Chemistry, Annamalai University, Annamalainagar 608 002,Tamil Nadu, India.
[b]Department of Chemistry, Central University of Tamil Nadu, Thiruvarur 601101,Tamil Nadu, India.

New symmetrical N,Nǿ-di(octadecyl)perylene-3,4,9,10-tetracarboxylic bisimide (DPBI) was synthesized and characterized by various spectral techniques. DPBI was highly fluorescent and exhibited strong absorption and emission in the visible spectral region. The self-assembly of DPBI was performed in a binary solvent CHCl$_3$/CH$_3$OH (40:60), which enable effective molecular aggregation. The molecule self-assembled as molecular wires and the self-assembled structure was analyzed using SEM, optical and fluorescence microscopic techniques. DPBI loaded TiO$_2$ catalyst was prepared in chloroform under sonication method using pure TiO$_2$. Newly prepared DPBI loaded TiO$_2$ was characterized and its photocatalytic activity has been tested for the degradation of Reactive Orange 4 (RO 4) using UV and solar light. The photocatalytic activity of DPBI loaded TiO$_2$ is higher than pure TiO$_2$ under UV and solar processes for the degradation of RO 4.The DPBI loaded TiO$_2$ is found to be reusable.

Introduction

Molecules of perylene tetracarboxylic diimide (PTCDI) form a unparalleled class of n-type organic semiconductor,[164] in comparison to the more common p-type counterpart. Bulk-phase materials of PTCDI have been extensively used in the fabrication of various optoelectronics devices.[5] Typical examples include thin-film transistors,[6,7] photovoltaics,[8] liquid crystals[9] and light-emitting diodes (LEDs).[10,11] PTCDI molecules attracted increasing interest in fabrication of single-molecule devices such as fluorescence switches,[12] sensors,[13,14] molecular wires, and transistors.[2,3] PTCDI is an excellent candidate for producing self-organized molecular electronic

materials due to its strong, well-studied π-π interactions. Depending on the substituent, perylene derivatives can exist in a wide range of hues and they provide yellow, orange, red, bordeaux, brown, and even black shades.[15] All these properties of this family of molecules largely depend on the nature and position of substituent attached to the main perylene board and on the matrix in which they are embedded.[16-18] Various types of new PTCDI molecules are synthesized for numerous applications in modern electronics.

TiO_2 is the most popular photocatalyst for environmental remediation because it is non-toxic, chemically stable and inexpensive. It can also be used as a functional material, adsorbent, cosmetics, and gas sensor.[19-21] But the photocatalytic activity of TiO_2 is constrained by its wide bandgap (3.03 eV for rutile and 3.18 eV for anatase) and fast electron-hole recombination.[22-25] Therefore increasing the photocatalytic activity in the visible region is still a principal challenge in this research field. The introduction of visible light active materials into TiO_2 should be a possible approach for improving its solarphotocatalyticactivity.[26] The main advantage of this approach, that bears similarities to dye-sensitized nanocrystalline titanium dioxide solar cells[27] is that the interfacial area between the *p-* and *n*-type materials is increased extremely, resulting in a more efficient charge generation and improved use of the solar radiation. Perylene and perylene diimide compounds are widely utilized synthetic dyes. They were applied initially as vat dyes and pigments due to their chemical inertness as well as their broad range of colours, red to violet and even black.[5] PTCDI is a cheap organic dye with strong absorption in the visible region, having high photo- and thermal stability.[28] PTCDI, as a typical n-type semiconductor, has higher electron affinity [LUMO] and electron mobility due to its strong   -   stacking between the conjugated bond. As a result, PTCDI materials are extensively employed as fluorescent and near-infrared dyes and in organic field effect transistors, photoinduced diodes.[29-32]

Remarkable energy conversion efficiencies have been obtained with organic dyes such as perylene derivatives and they are extensively used in photovoltaic devices, light emitting diodes

due to high molar absorptivity, high quantum yields etc.[33,34] N,Nʹ-Dialkyl-(diaryl) imides of perylene tetracarboxylic acids are important dyes or pigments of high thermal as well as photochemical stability. Photosensitization and photcatalysis studies involving electron transfer reactions between visible light absorbing molecules (PTCDI derivatives) and wide band gap n-type metal oxide semiconductor nanoparticles (TiO_2, SnO_2, and ZnO) have been widely studied because of its application in dye sensitized solar cells (DSSCs) for solar energy conversion and effective environmental remediation. Recently, binding ability of perylene diimides with SnO_2 and TiO_2 nanoparticles has been reported.[35] In continuation of our work on modified TiO_2 photocatalysts,[36-38] we designed and synthesized a new highly fluorescent N,Nʹ-di(octadecyl)perylene-3,4.9,10-tetracarboxylic bisimide(DPBI) **(Scheme 1)**and DPBI loaded TiO_2.Self-assembly, photochemical, thermal and electrochemical properties of DPBI have been investigated. The photocatalytic activity of newly prepared DPBI loaded TiO_2 has been tested for the degradation of Reactive Orange 4 (RO 4) using UV and solar light.

2. Experimental section

Materials and measurements

Perylene-3,4,9,10-tetracarboxylic dianhydride, imidazole and n-octadecylamine, titanium isopropoxide, isopropanol were obtained from Aldrich and used as received. Tetraisopropylorthotitanate was purchased from Himedia.^{1}H and ^{13}C NMR spectra were recorded in $CDCl_3$ at $50^{\circ}C$ temperature using BRUKER AMX-500 MHz. The chemical shift was assigned in ppm using the solvent signal as a reference. FT-IR spectra were recorded using the KBr method with NICOLET 6 AVATAR 360 FT-IR spectrophotometer. Mass spectrum was recorded on JEOL-GC mate mass spectrometer. UV-vis absorption spectra were recorded on a HITACHI U2001 UV-vis spectrophotometer. Fluorescence spectra were recorded by using ELICO SL-174 spectrofluorimeter. Differential Scanning Calorimetry was performed using DSC Q20 V24.2. Cyclic voltammetry was performed using three-electrode cell units, with polished 2-mm glassy

carbon as working, platinum as counter and Ag/AgCl as reference electrode in CHI604C-electro chemical analyzer. TBAP was used as supporting electrolyte. Scan rate of 100 mVs^{-1} and current sensitivity of 0.01mA were employed. The E_{HOMO} and E_{LUMO} energy were calculated using B3LYP level of DFT using 3-21G basis set. The scanning electron microscopy (SEM) images were taken with a HITACH S-3400N microscope. The sample was prepared by casting a methanol solution of the compound (25mm aged 1h) onto a clean glass side, followed by drying in air. The air-dried glass slide was then annealed overnight in an oven at 45°C. The sample was coated with gold before SEM measurement. Fluorescence microscopic image was recorded with LEICA BM-2500 microscope. Optical microscopic image was performed with a system based on a LABOMED ATC-2000 optical microscope. The pH of the solution was measured by ELICO (H-10T model) digital pH meter.

Photodegradation studies - Irradiation procedure

For the degradation by UV-A light (365 nm), a Heber Multilamp-photoreactor HML MP 88 was used.[39] This model consists of 8W medium pressure mercury vapour lamps set in parallel with emission at 365 nm wavelength. It has a reaction chamber with specially designed reflector made of highly polished aluminium and built in cooling fan. Also, provided with a magnetic stirrer and 50 mL reaction glass tubes. The light exposure length is 330mm. The irradiation was carried out using four parallel 8W medium pressure mercury lamps. The solution with catalyst and dye was continuously aerated by a pump to provide oxygen and to mix the solution.

Fifty millimeters of RO 4 (5×10^{-4} M) with the appropriate amount of catalyst was stirred for 30 min in the dark prior to illumination in order to achieve maximum adsorption of RO 4 onto the semiconductor surface. During the illumination time no volatility of the solvent was observed. At specific time intervals 2-3 mL of sample was withdrawn and catalyst was removed by centrifugation. The changes in the concentration of RO 4 were monitored from its characteristic absorptions at 285 and 489 nm using UV-visible spectrophotometer. The absorbance at 489 nm is

used to monitor the decolourization of RO 4. The absorbance at 285 nm represents the aromatic part of RO 4 and its decrease indicates the degradation of aromatic part of dye.

Solar light intensity measurements

Solar light intensity was measured for every 30 min and the average light intensity over the duration of each experiment was calculated. The sensor was always set in the position of maximum intensity. The intensity of solar light was measured using LT Lutron LX-10/A Digital Lux meter and the intensity was $1250 \times 100 \pm 100$ Lux.

Synthesis of N,N′-di(octadecyl)-perylene-3,4,9,10-tetracarboxylic diimide (DPBI)

In a 100mL round bottom flask, Perylene-3,4,9,10-tetracarboxylic dianhydride, (0.784g, 2mmol), n- octadecylamine (1.078g, 4mmol) and imidazole (4g) were added and refluxed at 140 °C for 3h. The reaction mixture was cooled to room temperature and dispersed in 100 mL ethanol followed by addition of 300mL 2M HCl. The mixture was stirred overnight. The resulting dark-red solid was filtered off and washed thoroughly with distilled water. The collected solid was dried at 100°C under vaccum and the yield was 89%.
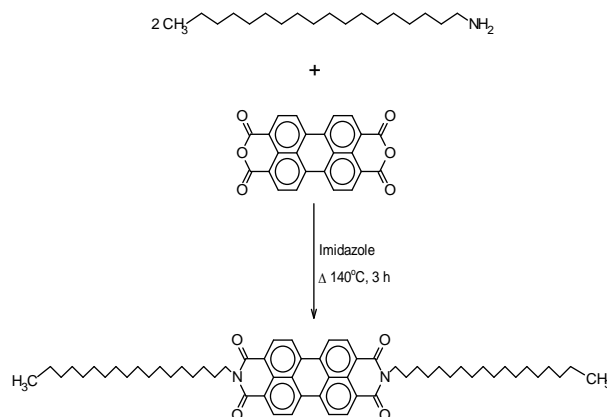
Scheme 1 Synthesis of N,N'-di(octadecyl)perylene-3,4.9,10-tetracarboxylic bisimide (DPBI).

Structure of the product was confirmed by spectral data which is given below.

FT-IR, cm^{-1} (KBr): 2922 vs 2848s [$_{(C-H)}$ aliphatic], 1696 vs 1656s [$_{(C=O)}$], 1592 [s $_{(C=C)}$], 1345 [s $_{(C-N)}$], 1252w, 1089w [$_{(C-H)}$ aromatic bending], 851w, 808s, 746s [$_{(C-H)}$ aromatic wagging] (br, broad; s, strong; m, medium; w, weak). MS: m/z calcd for $C_{60} H_{82} N_2 O_4$: 894: found 894.5. ^{1}H NMR: (50 °C, 500MHz CDCl$_3$): 8.6 (4H d, perylene, J=10Hz), 8.61 (4H, d, perylene, J=5Hz), 4.2 (4H, t, N-CH$_2$), 1.77, 1.76, 1.74, 1.38, 1.26 (64H, m, CH$_2$), 0.89 ppm. (6H, t, CH$_3$) ^{13}C NMR (50 °C, 500MHz, CDCl$_3$): 163 (C=O, 139, 131, 130, 128, 127, (perylene), 38 (N-CH$_2$), 33, 31, 29, 28, 22 (CH$_2$), 14 (CH$_3$) ppm.

Preparation of TiO$_2$

The TiO$_2$ was prepared by the reported procedure.[40] The TiO$_2$ was prepared by sol-gel method, taking tetraisopropylorthotitanate (Himedia 98%) as the starting material. 12.5 ml of tetraisopropylorthotitanate was dissolved in 100 mL of 2-propanol (Spectrochem×99.5%) and to this solution 3mL of water was added drop wise under vigorous stirring. The resulting colloidal suspension was stirred for 4h. The gel obtained was filtered, washed and dried in an air oven at 100°C for 5 h. The sample was calcinated at 400°C in a muffle furnace for 12h.From the XRD results, the prepared TiO$_2$ is in anatase phase and crystalline size of prepared TiO$_2$ is determined using Debye–Scherrer eqn.1.

$$D = K \lambda / \beta \cos \theta \quad\quad \ldots (1)$$

Where D is the Crystal size of the catalyst, K is dimensionless constant, is the wavelength of X-ray, is the full width at half-maximum (FWHM) of the diffraction peak and is the diffraction angle. The average crystalline size of prepared TiO$_2$ is found to be 15.2 nm.

Sonochemical preparation of DPBI loaded TiO$_2$

About 4g of prepared TiO$_2$was suspended in 8 mL of chloroform and to this 2 mg of DPBI dissolved in2 mL of chloroform was added drop wise for 20 minutes under sonication. The resulting colloidal suspension was sonicated further for10 minutes. The gel obtained was

evaporated and dried in an air oven at 100°C for 1h. This catalyst contained 0.05wt% of DPBI.

Similarly catalyst with 0.2 wt% of DPBI was prepared with the same procedure.

Results and Discussion

Optical properties

The UV-vis absorption spectra of DPBI in $CHCl_3$ were recorded at different concentration (Fig. 1).

Spectrum shows three pronounced peaks in visible region at 458, 489, 526 nm and a shoulder

around 431 nm, which correspond to the 0-0, 0-1, 0-2 and 0-3 electronic transitions, respectively.

The fluorescence emission spectra of DPBI in $CHCl_3$ at various concentrations were recorded

with $_{exi}$= 460nm. The fluorescence emission peaks appeared at 533 and 574nm. The fluorescence

spectra depicts the same peak structure with the mirror image of the absorption, (Fig. 2) due to the

two nitrogen positions at the imides are node in π-orbitals.[41] This reveals the same geometry in

ground and excited states.

DSC Measurement

Thermal analysis of the DPBIwas studied by differential scanning calorimetry (DSC). The

thermogram of DPBI exhibits three endothermic peaks at 141.60 °C, 177.34 °C and 307.13 °C

during the heating (Fig. 3). The first two peaks indicate a transition and the third is a typical

melting peak. A similar kind of broad transition was previously reported for PTCDI molecules.[42]

Electrochemistry

The cyclic voltammogram of DPBI was recorded in DMF using tetrabutylammonium

perchlorate (TBAP) as the supporting electrolyte (Fig. 4). The voltammogram was recorded with

ascan rate of 100 m V s^{-1}.The cyclic voltammetric curve shows a reversible one-electron

reduction peak at ό0.543 V. This value is considerably less negative than the reduction properties

of perylene carboxylate (aromatic core of PTCA showed a pair of reversible redox peaks at ca. ό

1.68 V). [43,29-32] The compound has perylene ring and electron-withdrawing imide groups and thus

electrons can be transferred from molecule to molecule coupled by weak van der Waaløs forces. Hence, the compound can be used as an organic semiconductor.

Theoretical calculations

The calculated HOMO and LUMO energies of DPBI are ó0.2268 and ó0.1355 a.u. respectively. The DPBI is a stronger electron acceptor than perylene carboxylate because of the lack of electron-withdrawing diimide fragment in perylene carboxylate (HOMO and LUMO energies of PTCDA are ó9.33 eV and ó2.95 eV, respectively).[44, 29-32] HOMO-LUMO pictures of the optimized structure of DPBI are presented in Fig. 5.

Morphology characterization of self-assembly from solution

Fig. 6 shows optical photographs capturing the progression of self-assembly of DPBI as molecular aggregation. The self- assembly of the molecules occurred at the interface between a õpoorö (methanol) and õgoodö (chloroform) solvent. The bottom layer of the vials contains DPBI dissolved in $CHCl_3$ and the upper layer contains CH_3OH. An initial swirl of the vial immediately induced the supramolecular self-assembly and in 30 minutes, the complete formation of molecular wires was observed. Self-assembly approach takes the advantage of the strong intermolecular - interaction, which is enhanced in a solvent where the molecule has minimum interactions with the solvent. Fluorescence microscopy image of DPBI aggregate deposited on glass is shown in Fig 7a (wavelength of excitation: 450 nm; emission: >515 nm). The aggregates were synthesized through phase-transfer between excessive CH_3OH and $CHCl_3$ solution (0.33 mM). The red emission was clearly seen at the aggregates. Fig. 7b shows an optical microscopy image of self-assemblies. The sample was prepared by casting the CH_3OH solution of aggregates on a glass coverslip (40:60 $CHCl_3$:CH_3OH).   The image shows molecular aggregates of DPBI formed on the surface of the substrate after solvent evaporation. This image also confirms the formation of molecular aggregates of almost uniform size. The SEM image of the molecular assembly spin-cast on glass shows particulate aggregates of

approximately wire shape with size of 200-1000 nm(width)(Fig 7c and 7d). The wire morphology of molecular aggregate is consistent with the distorted π-π stacking, which prevent the molecule from assembly along one dimension.

Characterization of DPBI loaded TiO$_2$

The DPBI loaded TiO$_2$ catalyst was characterized by its colour, FT-IR, DRS and SEM techniques. The colour of the pure TiO$_2$, 0.05 wt% DPBI loaded TiO$_2$ and 0.2 wt% DPBI loaded TiO$_2$ are shown in Figs. 8a, b and c, respectively. The pure TiO$_2$ is white in colour (Fig. 8a) whereas DPBI loaded TiO$_2$ is pink in colour (Figs. 8b and 8c). This indicates the presence of DPBI on the TiO$_2$ surface. The FT-IR spectra of pure TiO$_2$ and 0.05 wt% DPBI loaded TiO$_2$ are given in Figs. 9a and b, respectively. In DPBI loaded catalyst, new peaks characteristic of DPBI appeared at 1123 (w (CóH), 1336 (w (CóN)) and 2851, 2920 (s (CóH)) cm^{-1}(s, strong: w, weak). These peaks reveal the presence of DPBI in the catalyst.

The diffuse reflectance spectra of pure TiO$_2$ and 0.05 wt% DPBI loaded TiO$_2$ are displayed in Figs. 10a and b, respectively. The diffuse reflectance spectra reveal that the loading of DPBI in TiO$_2$ results in increased absorbance from 400 to 650nm. The structure and morphology of the catalyst are very important parameters as they influence the photocatalytic activity. The SEM images of pure TiO$_2$ and 0.05 wt% DPBI loaded TiO$_2$ are shown in Figs. 11a and b, respectively. Fig. 11b shows sponge like DPBI clusters embedded on the TiO$_2$ surface (see inset figure).

Photocatalytic activity of DPBI loaded TiO$_2$

The photocatalytic activity of the DPBI loaded catalyst was tested for the degradation of Reactive Orange 4 (RO 4). The Reactive Orange 4 azo dye (RO 4), (C.I. No. 18260, molecular formula: $C_{24}H_{13}N_6O_{10}C_{12}Na_3$, molecular weight: 781.21) is extensively used in dying industries. The dye has the adsorption maxima at 489 and 285 nm. The dye structure and UV-spectrum of RO 4 are given in Fig.S1 (see Supplementary data).

Photocatalytic degradation and decolourization of RO 4 with pure TiO_2, 0.05 wt% DPBI loaded TiO_2 and 0.2wt% DPBI loaded TiO_2 catalysts under UV light are shown in Fig. 12a. When the dye solution is irradiated without catalyst there is negligible degradation (0.2%) and for the same experiment when performed in the absence of light with 0.05 wt% DPBI loaded TiO_2, only 4.0% dye removal occurs. This decrease in dye concentration with 0.05 wt% DPBI loaded TiO_2 in the absence of UV light may be due to the adsorption of dye on the catalyst. Dye undergoes 84.6% degradation and 97.7% decolourization in presence of 0.05 wt% DPBI loaded TiO_2 catalyst and UV light at 60 min irradiation whereas with pure TiO_2 only 44.5% degradation and 83.3% decolourization occurred. These observations reveal that both UV light and photocatalyst are needed for effective destruction of RO 4. There is no significant change with 0.2 wt% DPBI loaded TiO_2. Degradation efficiency of 0.05 wt% DPBI loaded TiO_2 is almost twice that of pure TiO_2. This shows that UV/0.05 wt% DPBI loaded TiO_2 is more efficient in RO 4 degradation than pure TiO_2.

The Fig. 12b shows the photocatalytic degradation of Reactive Orange 4 with pure TiO_2, 0.05 wt% DPBI loaded TiO_2 and 0.2 wt% DPBI loaded TiO_2 catalysts under solar light. The trend observed in solar light is same as in UV light. Dye undergoes 61.2% degradation and 82.4% decolourization in presence of 0.05 wt% DPBI loaded TiO_2 catalyst and solar light at 60 min irradiation whereas with pure TiO_2 only 37.8% degradation and 69.5% decolourization are observed. The results show that 0.05 wt% DPBI loaded TiO_2 is more efficient in RO 4 degradation than pure TiO_2 in solar light. The efficiency in UV process is higher than that of solar process with 0.05 wt% DPBI loaded TiO_2.

The stability of the 0.05 wt% DPBI loaded TiO_2 has been tested towards RO 4 degradation under UV light with three successive cycles (Fig. S2, see Supplementary data). After the each run, the catalyst was recovered, washed with water and dried in an air oven at 100°C for 1h. The

degradation efficiency was 81.2% even at third run. These results indicate that DPBI loaded TiO$_2$remains effective and reusable.

The UV-vis spectra of RO 4 (5 $\times 10^{-4}$ M) solution at different irradiation times with UV light are shown in Fig. S3(see Supplementary data). The absorption peaks in UV and visible regions decreases gradually and finally disappear indicating the complete degradation of the dye. There is no significant change in spectra during irradiation and the intensity at 285 and 489 nm decreases during the degradation. This reveals that the intermediates do not absorb at the analytical wavelengths of 285 and 489 nm.

Conclusions

The Symmetrical N,Nⱷ-di(octadecyl)perylene-3,4.9,10-tetracarboxylic bisimide was synthesized and characterized. Its photophysical, thermochemical and electrochemical properties were analysed. The molecular self-assembly was observed in CHCl$_3$/CH$_3$OH mixture, and in 30 minutes, the complete formation of molecular wires was observed. The compound with high photostability, and absorption and emission maxima above 500 nm enables it to be exploited as a high-performance fluorescence marker in aqueous media. DPBI loaded TiO$_2$ prepared by sonochemical method, is more efficient in RO 4 degradation than pure TiO$_2$ in UV and solar light. The efficiency in UV process is slightly higher than that of solar process.
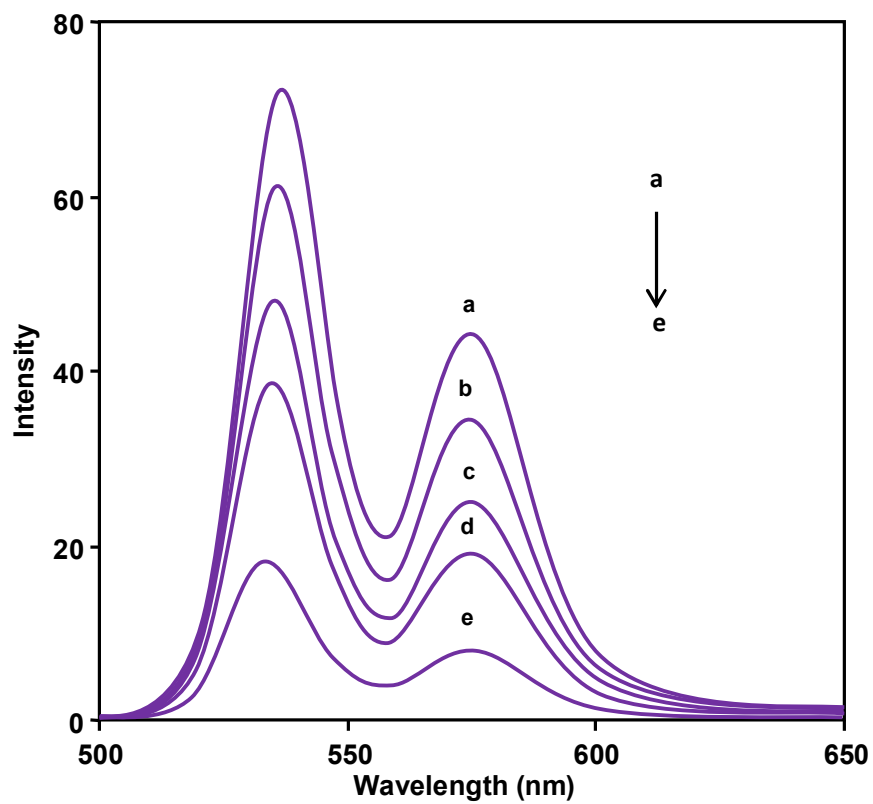
Acknowledgments

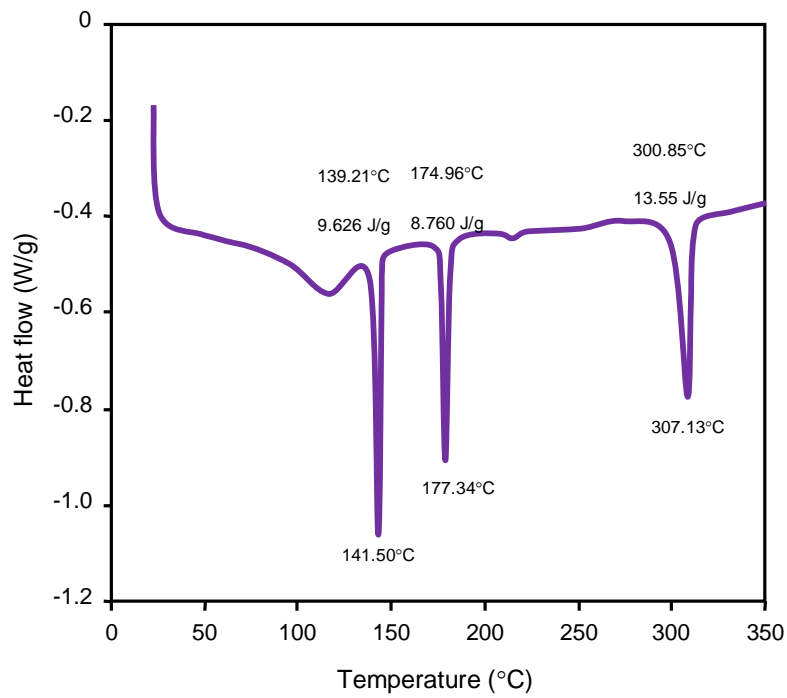**Electronic supplementary information (ESI) available. Figs. S1-S3**
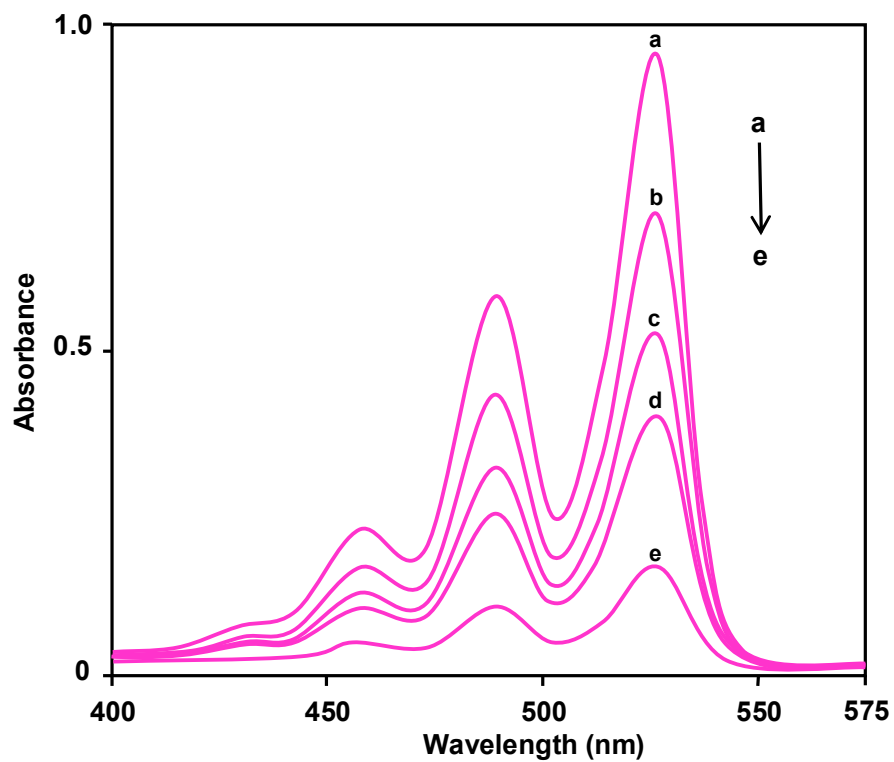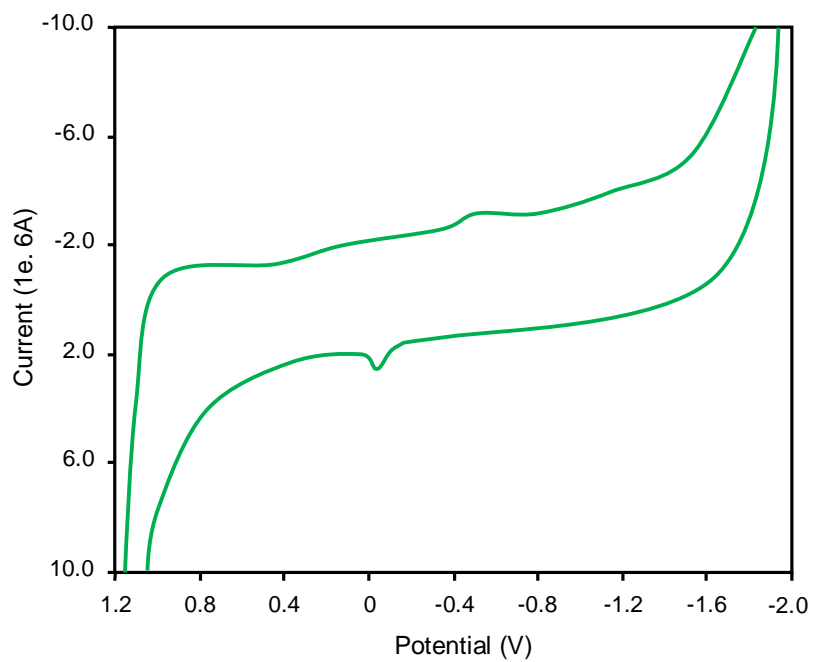
Fig. 1 UV-Vis spectra of DPBI in CHCl$_3$
a) 1.5×10^{-5}, b) 1.0×10^{-5}, c) 0.7×10^{-5}, d) 0.5×10^{-5} and e) 0.2×10^{-5} mol/L
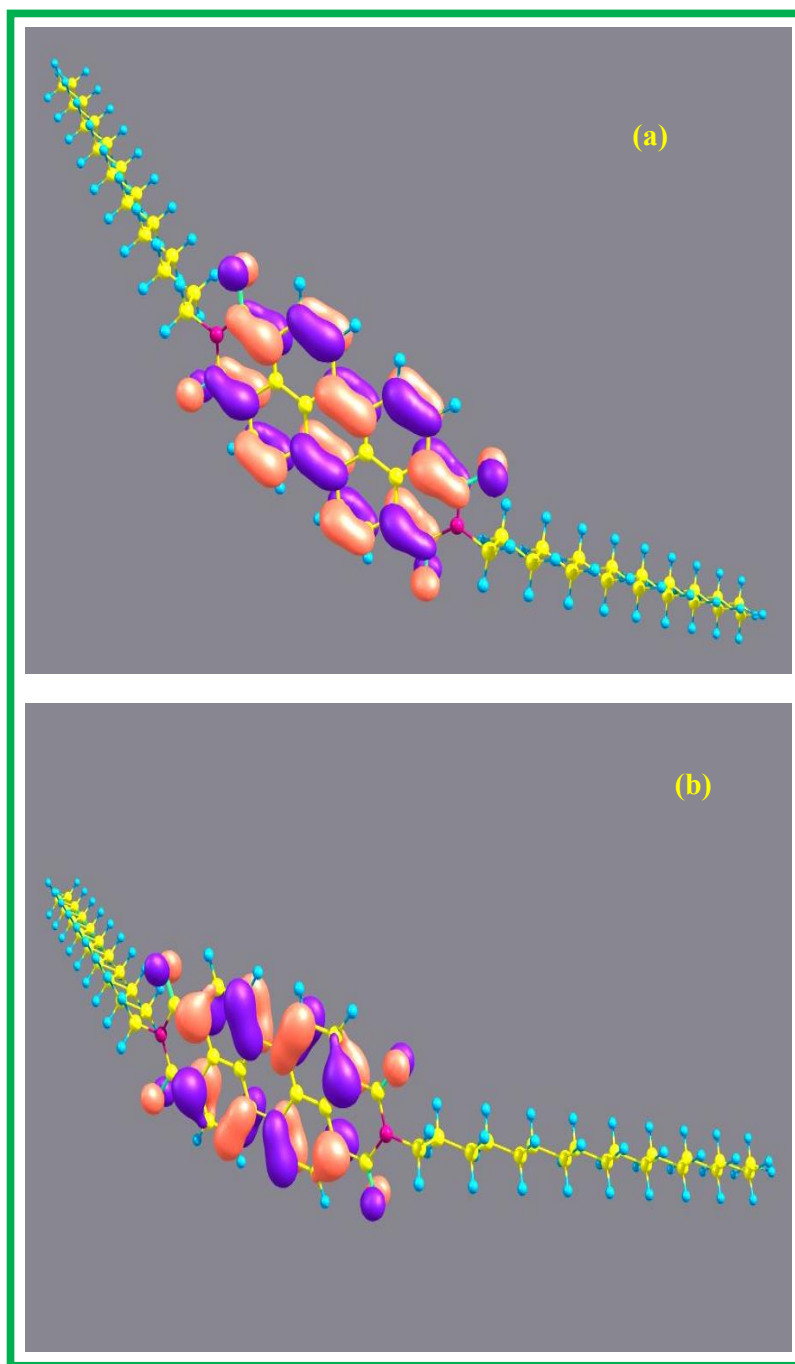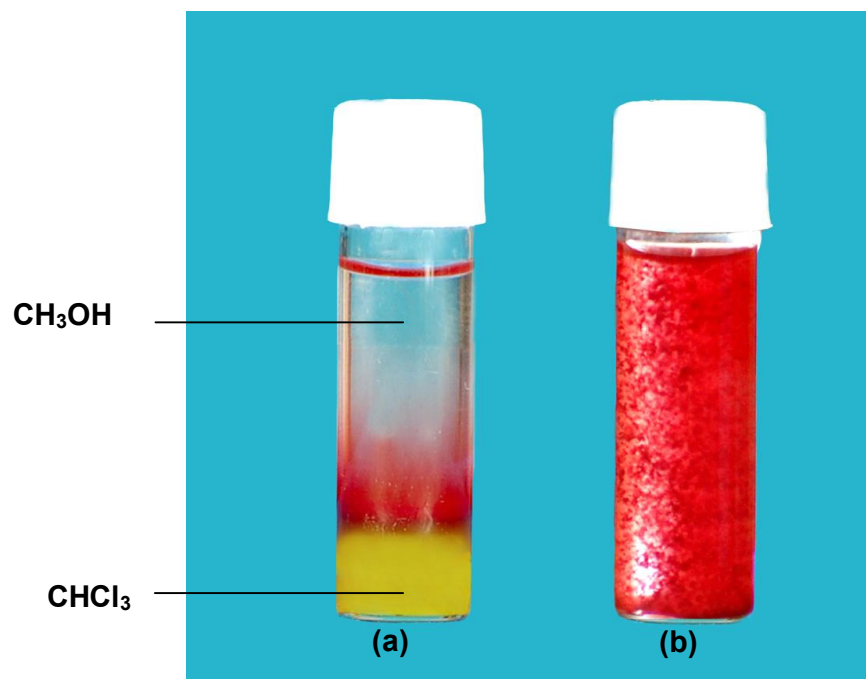
Fig. 2 Fluorescence spectra of DPBI in CHCl$_3$

a) 1.5×10^{-5}, b) 1.0×10^{-5}, c) 0.7×10^{-5}, d) 0.5×10^{-5} and e) 0.2×10^{-5} molL^{-1}

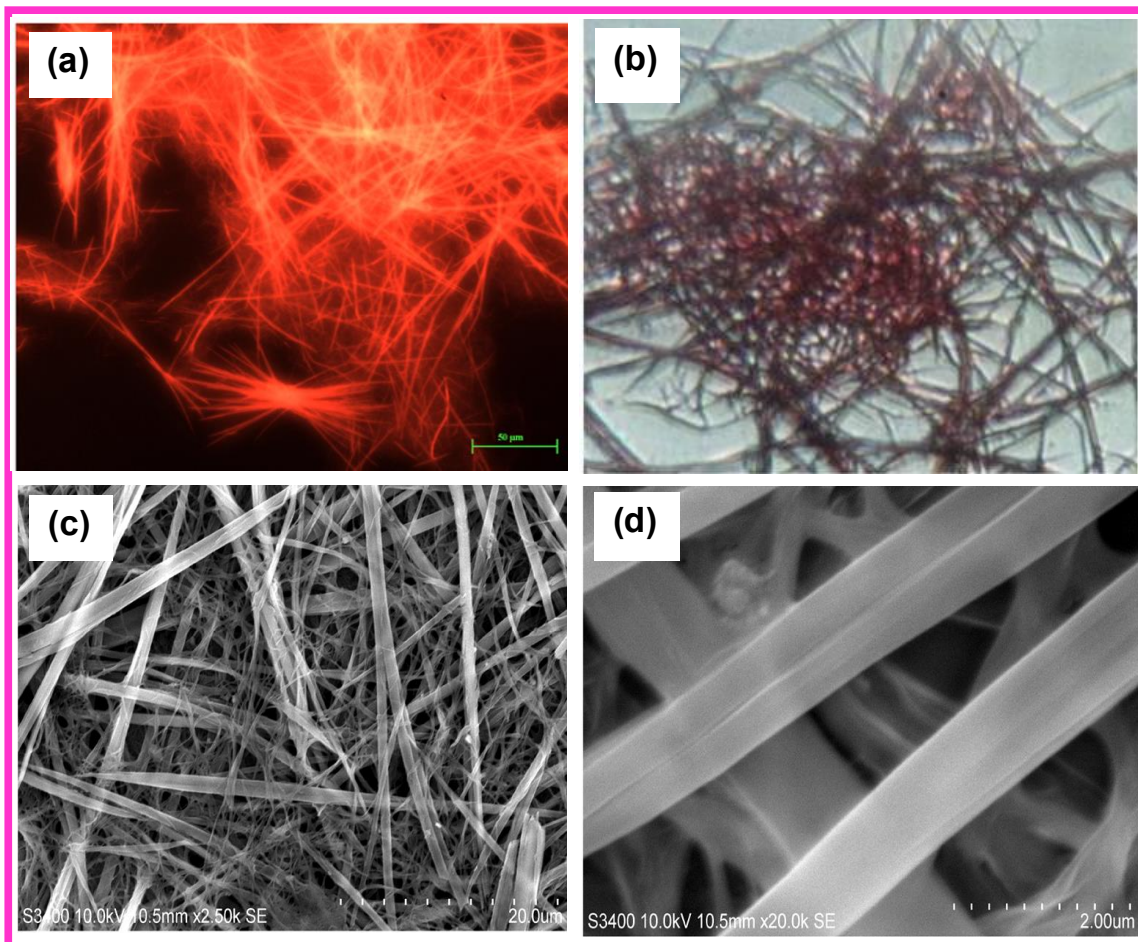**Fig. 3** DSC thermogram of DPBI

16

Fig. 4 Cyclic voltammogram of DPBI in DMF

Fig. 5 a) HOMO orbital of DPBI b) LUMO orbital of DPBI

**Fig. 6** Molecular aggregation of DPBI in CHCl₃/CH₃OH: (a) 0 min and (b) after 30 min

Figs. 7 (a) Fluorescence microscopic image (molecular wires(50 m)) of DPBI
(b) Optical microscopic image (molecular aggregates) of DPBI
(c) SEM image Molecular wires (20 m) (lower magnification) and
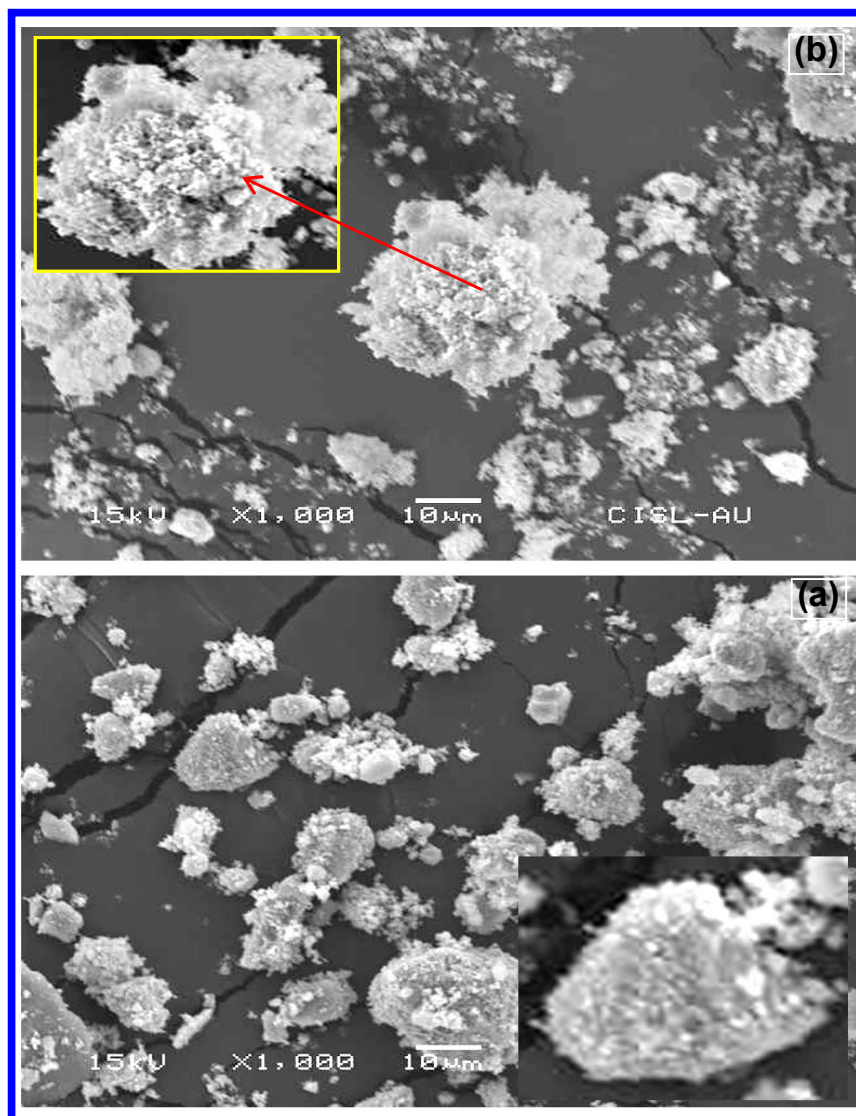**(d)** Molecular wires (2 m) (Higher magnification)
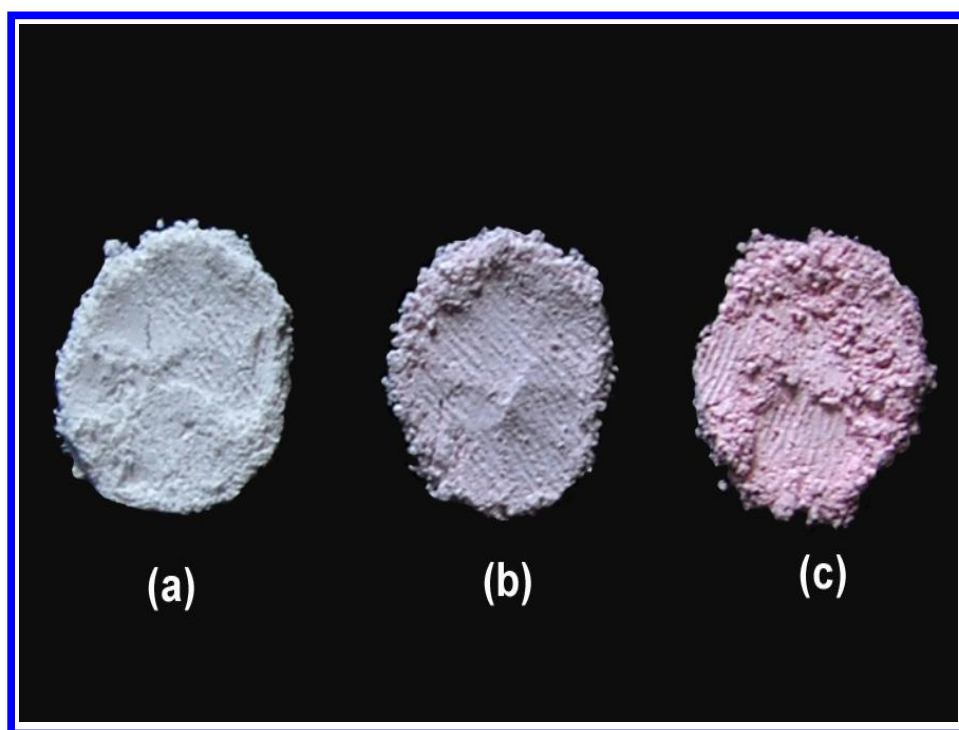
Fig. 8 Colour of a) pure TiO$_2$, b) 0.05 wt% of DPBI loaded TiO$_2$ and c) 0.2 wt% of DPBI loaded TiO$_2$
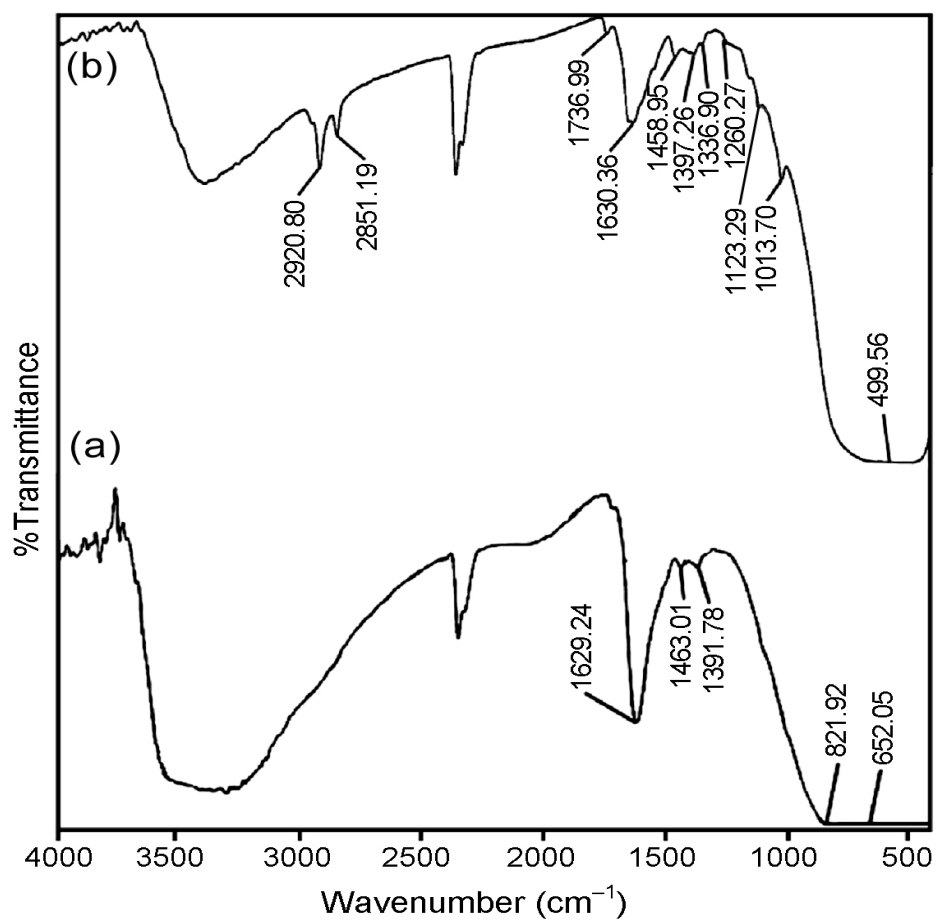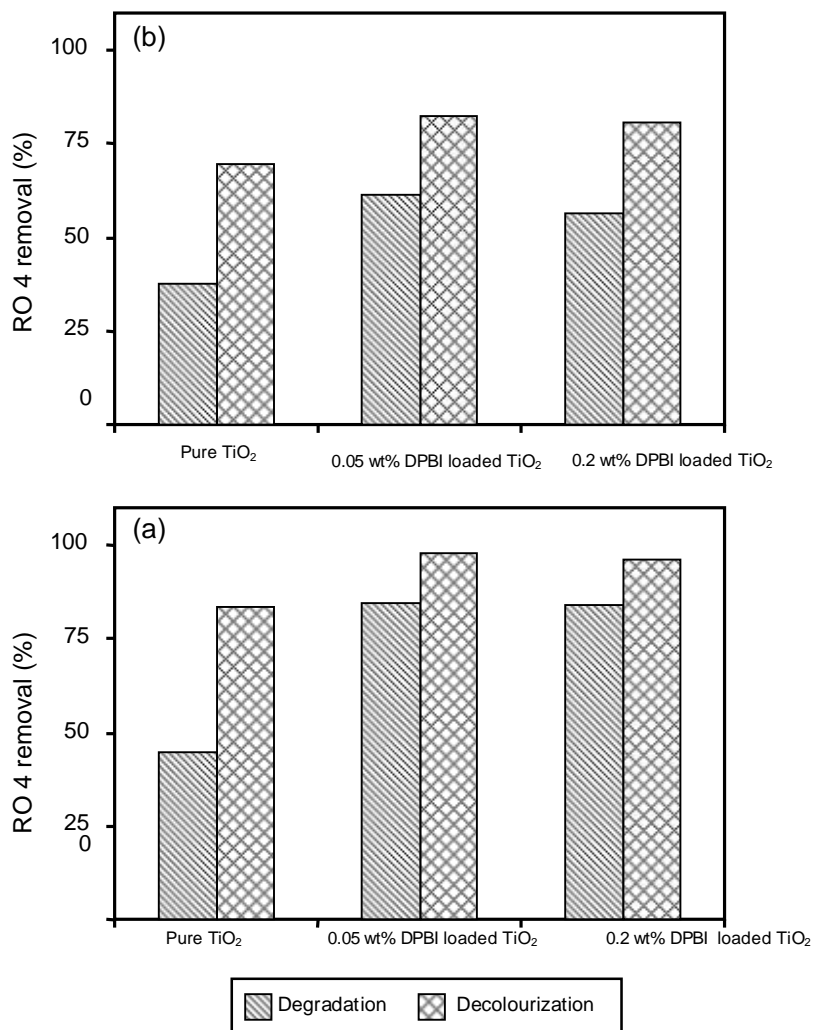
Fig. 9 FT-IR spectra of a) pure TiO_2 and b) 0.05 wt% of DPBI loaded TiO_2
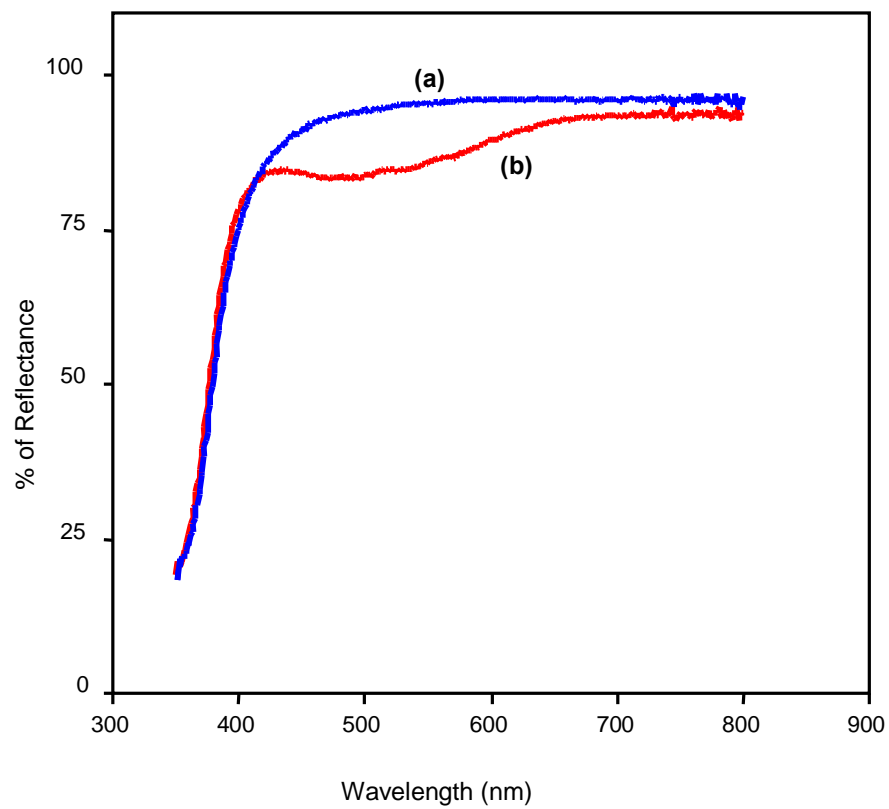
Fig. 10 DRS of a) pure TiO_2 and b) 0.05 wt% of DPBI loaded TiO_2

Fig. 11SEM image of a) Pure TiO$_2$ and b) 0.05 wt% of DPBI loaded TiO$_2$

Fig. 12 Photodegradation and decolourization of RO 4:
a) UV process and b) solar process
[RO 4] = 5 ×10⁻⁴M, pH = 7, catalyst suspended = 2gL⁻¹,
airflow rate = 8.1   mLs⁻¹, I$_{UV}$= 1.381× 10⁻⁶einstein L⁻¹ s⁻¹

Notes and references

1. O. Boudrioua, H. Yang, Ph. Sonnet, L. Stauffer, A. J. Mayne, G. Comtet, G. Dujardin, Y. Kuk, S. Nagarajan, A. Gourdon and E. Duverger, Physicalrev. *B* 2012, *85,035423.*

2. H. Yang , O. Boudrioua, A. J. Mayne, G. Comtet, G. Dujardin , Y. Kuk, Ph. Sonnet, L. Stauffer , S. Nagarajan and A. Gourdon, Phys. Chem. Chem. Phys. 2012, **14**, 1700.

3. G. Boobalan, P K M. Imran and S. Nagarajan, Superlattices and Microstructures. 2012, **51,** 921.

4. G.Boobalan, P K M Imran and S.Nagarajan, Supramol. Chem.*,*2012, *24 238.*

5. F. Wurthner, Chem. Commun., 2004, **14**, 1564.

6. R.J. Chesterfield, J.C. McKeen, C.R. Newman, P.C. Ewbank, D.A. da Silva Filho, J.L. Bredas, L.L. Miller, K.R. Mann and C.D. Frisbie, J.Phys. Chem. B 2004, **8**, 19281.

7. B. A. Jones, M. J. Ahrens, M. H. Yoon, A. Facchetti, T. J.Marks and M. R. Wasielewski, Angew. Chem., Int. Ed. 2004, **43**, 6363.

8. B. A. Gregg, J. Phys. Chem. B, 2003, **107**, 4688.

9. C. W. Struijk A. B. Sieval, J. E. Dakhorst, M.Van Dijk, P. Kimkes, R. B. Koehorst, H. Donker, T. J. Schaafsma, S. J.Picken, A. M. Van de Craats, J. M. Warman, H. Zuihof and E. J. R. Sudholter, J. Am. Chem. Soc., 2000, **122**, 11057.

10. S. Alibert-Fouet, S. Dardel, H. Bock, M. Oukachmih, S. Archambeau, I. Seguy, P. Jolinat and P. Destruel, Chem. Phys. Chem. 2003, **4**, 983.

11. P. Schouwink, A.H. Schafer, C. Seidel and H. Fuchs, Thin Solid Films 2000, **372**, 163.

12. R. Gronheid, A. Stefan, M. Cotlet, J. Hofkens, J. Qu, K. Muellen, M. van der Auweraer, J.W. Verhoeven and F.C. De Schryver, Angew. Chem. Int. Ed. 2003, **42**, 4209.

13. M.W. Holman, R. Liu, L. Zang, P. Yan, S.A. DiBenedetto, R.D. Browers and D.M. Adams, J. Am. Chem. Soc. 2004, **126**, 16126.

14. C. Carimsdal Andrew and K. Mullen, Angew. Chem. Int. Ed. 2005, **44**, 5592.

15. M. Herbst and K. Hunger, Industrial Organic Pigments, VCH, New York, 1993.

16. J. Ferguson, J. Chem. Phys. 1996, **44**, 2677.

17. A.K. Dutta, K. Kamada and K. Ohta, Langmuir, 1996, **12**, 4158.

18. S. Akimoto, A. Ohmori and I. Yamazeki, J. Phys. Chem. B 1997, **101**, 3753.

19. Y. F. Chen C. Y. Lee, M. Y. Yeng and H. T. Chiu, J. Cryst. Growth 2003, **247**, 363.

20. AB. Corradi, F. Bondioli, B. Focher, A. M. Ferrari, C. Grippo, E. Mariani and C. Villa, J. Am. Ceram. Soc. 2005, **88,** 2639.

21. Z. Zhang, X. Zhong, S. Liu, D. Li and M. Han, Angew. Chem. Int. Ed 2005, **44**, 3466.

22. B. Tryba, IntJ. Photoenergy.. 2008, **2008**, 15.

23. H. Ding, H. Sun and Y. Shan, J. Photochem. Photobiol., A 2005, **169**, 101.

24. K. Ajito, J. P. H. Sukamto, L. A. Nagahara, K. Hashimoto and A. Fujishima, J. Electroanal. Chem. 1995, **386**, 229.

25. X. Zhang, K. Udagawa, Z. Liu, S. Nishimoto, C. Xu, Y. Liu, H. Sakai, M. Abe, T. Murakami and Fujishma, J. Photochem. Photobiol., A 2009, **202**, 39.

26. H. Kyung, J. Lee and W. Choi, Environ. Sci. Technol., 2005, **39**, 2376.

27. B. O∅Regan and M. Gratzel, Nature, 1991, **355**, 737.

28. H. Icil, D. Uzun and E. Arslan, Spectrosc. Lett. 2001, **34**, 605.

29. H. Icil and E. Arslan, Spectrosc.Lett.2001, **34**, 355.

30. C. D. Dimitrakopoulos and P. R. L. Malenfant, Adv. Mater, 2002, **14(2)**, 99.

31. B.F. Zhang, E. Perzon, X. Wang, W. Mammo, M. R. Andersson and O. Inganas, Adv Funct. Mater. 2005, **15(5**), 745.

32. L. Schmidt-Mende, A. Fechtenkotter, K. Mullen, E. Moons, R. H. Friend and J. D. MacKenzie, Science, 2001, **293**, 1119.

33. C. Li, J. Yum, S. Moon, A. Herrmann, F. Eickemeyer, N.G. Pschirer, P. Erk, J. Schöneboom, K. Müllen, M. Grätzel and M.K. Nazeeruddin, ChemSus Chem. 2008, **1,** 615.

34. R. Abbel, C. Grenier, M.J. Pouderoijen, J.W. Stouwdam, P.E.L.G. Leclere, R.P. Sijbesma, E.W. Meijer and A.P.H.J. Schenning, J. Am. Chem. Soc. 2009, **131,** 833.

35. G. Paramaguru, N. Nagarajan and R. Renganathan, J. Mol. Struct. 2013, **1038,** 235.

36. B. Subash, B. Krishnakumar, R.Velmurugan and M. Swaminathan, Sep. Purif. Technol. 2012, **101**, 106.

37. R. Velmurugan, B. Krishnakumar, B. Subash and M. Swaminathan, Sol. Energy Mater. Sol.Cells 2013, **108**, 212.

38. N. Sobana, M. Muruganadham and M. Swaminathan, J. Mol. Catal. A: Chem. 2006, **258**, 132.

39. M. Muruganandham and M. Swaminathan, Dyes Pig, 2006, **68**, 133.

40. R. Velmurugan, B. Krishnakumar, R. Kumar and M. Swaminathan, Arabian. J. Chem. 2012, **5**, 447.

41. H. Langhals, Heterocycles. 1995, **40**, 477.

42. Z. Chen, U. Baumeister, C. Tschierske and F. Wurthner, Chem. Eur. J. 2007, **13**, 450.

43. M. Wang, F. N. Xiao, K. Wang, F. B. Wang and X. H. Xia, J. Electroanal. Chem. 2013, **688**, 304.

44. X. Zhang, Y. Wu, J. Li, F. Li and M. Li, Dyes Pigm. 2008, **76**, 810.